



HYDRODYNAMIC AND THERMAL TWO DIMENSIONAL BOUNDARY LAYERS DEVELOPMENT BETWEEN ROTATING TURBINE BLADES

Asst. Prof. Dr. Ihsan Y. Hussain
Mech. Engr. Dept.
College of Engineering
University of Baghdad
Baghdad – Iraq

Taif H. Salih
Mech. Engr. Dept.
College of Engineering
University of Baghdad
Baghdad – Iraq

ABSTRACT

The hydrodynamic and thermal boundary layers have great effect on the fluid flow and heat transfer between rotating turbine blade. In the present work, the flow and heat transfer is analyzed numerically by solving two dimensional incompressible boundary layer equations. A ($k - \epsilon$) turbulence modeling is used to obtain the eddy viscosity. The finite volume method is introduced to carryout all computational solution with staggered grid arrangement. Due to complex physical domain the original coordinate system is transferred to non orthogonal coordinate system. The calculation of present work done for rotating two dimensional turbine cascade with different rotating speeds (1500 rad/s, 1800 rad/s, 1900 rad/s), and for different Reynolds number (5000, 10000, 100000), in subsonic flow ($M < 1$). The two dimension fluid flow is described by presenting plots of vector and contour mapping for the velocity; pressure and heat transfer fields as well as Nusselt number variation. The results were verified through a comparison with published duct results, good agreement was obtained. The final results were then compared with published results for turbine blades and good agreement was also obtained, the overall comparison show good agreement.

الخلاصة

الطبقة المتاخمة الهيدرو ديناميكية والحرارية لها تأثير كبير على الجريان وانتقال الحرارة بين ريش التوربين الدوارة. في البحث الحالي تم تحليل الجريان وانتقال الحرارة عددياً بحل معادلات الطبقة المتاخمة ثنائية البعد اللانظغاطية. تم استخدام نموذج ($k - \epsilon$) للاضطراب للحصول على اللزوجة الدوامية. تم استخدام المربعات الكارتيزية للسرعة والضغط كمتغيرات معتمدة في معادلة الزخم. طريقة الحجوم المحددة تم استخدامها مع الشبكة المرحلة (staggered grid). بسبب التعقيد في المجال الفيزيائي للمسئلة، تم تحويل نظام الاحداثيات غير المتعامدة. تم حل معادلة الطبقة المتاخمة الهيدرو ديناميكية مع معادلة الطاقة في المجال العددي للمسئلة. تم استخدام طريقة SIMPLE للجريان اللانظغاطي للحصول على الحل وتفصيله خلال ريشتي توربين دوارة تم ايجاد الحل لثلاث سرع دورانية (1500 rad/s , 1800 rad/s, 1900 rad/s) ولثلاث قيم من رقم رينولدز (5000 , 10000 , 100000). تم اعداد برنامج باستخدام (power station) لتنفيذ الحسابات المطلوبة. تم تمثيل الجريان الثنائي البعد برسم المتجهات وخطوط التساوي (contours) للسرعة والضغط ودرجات الحرارة، وكذلك تقييم رقم نسلت. تم تدقيق النتائج بمقارنتها مع نتائج منشورة للجريان داخل مجرى وتم الحصول على توافق جيد. بعد ذلك تمت مقارنة النتائج النهائية مع نتائج منشورة للجريان خلال ريش توربين، وتم الحصول على توافق جيد.

Keywords: Turbine Blades, Rotating, Flow, Heat transfer

INTRODUCTION

The axial flow turbine has two main elements; the stationary vane called nozzle and a turbine rotor. One of the most important aspects of the turbine property is to choose the suitable blade profile. In the three dimensional flow inlets boundary layer separates and forms a horseshoe (or leading edge) vortex, with one leg of the vortex in one aerofoil passage and the other leg in the adjacent passage. Thus in a cascade flow, the part of the secondary flow that is called the passage vortex.

The main objective of present work is to investigate the fluid flow and heat transfer between two rotating turbine blades. This will be done by solving the governing continuity, momentum, and energy equations together with the $(k - \epsilon)$ turbulence model, numerically by the finite volume method. An orthogonal curvilinear coordinate system that is rotating with the blade will be used. The development of both hydrodynamic and thermal boundary layers over the blade surface will also be considered. Many investigations have provide data for the flow between turbine blades. However, rather literature is available for flow analysis. Koya and Kotake studied numerically fully developed flow through aturbine stage. Dorfman applied Naveier Stocke equation for gas turbine, to gather with heat conduction. Gogzeh developed finite volume method and code for solving elliptic three dimensional fluid flows. Thomkens study the quazi three dimensional finite difference boundary layer analysis for rotating blade row

MODELING

The blade profile is analyzed in frame work of an orthogonal curvilinear coordinate system rotating with blade.

The geometry under consideration is an impulse turbine blade as represented in figure (1), although it represents a three dimensional flow problem, a suitable simplification by assuming the flow throw a cascade construction will reduce it to a two dimensional problem. The blade dimensions are:-

Axial chord, $b_x = 11.08$ in (0.2813m)

Chord / axial chord = 1.2242

Pitch / axial chord = 0.9555

Aspect ratio (span / axial chord) = 0.9888

$\beta_1 = 43.99^\circ$

$\beta_2 = 22.98^\circ$

In this problem the mean flow is considered to be steady, and the following assumptions were used

1. The corioles acceleration creates a pressure gradient normal to the blade surface (∂u) even though it's larger than in usual boundary layer calculation.
2. Assumption of zero pressure gradients across the boundary layer is adopted.
3. It will know assumed that the gradients of all flow property in the x_2 direction are zero $\frac{\partial}{\partial x_2} = 0$

This reduce the x_2 momentum equation with the other equations.

4. Incompressible subsonic fluid flow.
5. Pure impulse turbine blade is adopted with zero degree of reaction.
6. The boundary layer assume to be turbulent from the leading edge of the blade



According to the above assumptions and the flow forces the governing equations will be; (Tompkins, 1982);

Continuity:

$$\frac{\partial}{\partial x_1}(\rho u_1 h_2) + \frac{\partial}{\partial x_2}(\rho u_2 h_1) + \frac{\partial}{\partial x_3}(\rho u_3 h_1 h_2) = 0 \quad (1)$$

X₁ Momentum Eq. :

$$\begin{aligned} \frac{\rho u_1}{h_1} \frac{\partial u_1}{\partial x_1} + \frac{\rho u_2}{h_2} \frac{\partial u_1}{\partial x_2} + \rho u_3 \frac{\partial u_1}{\partial x_3} + \rho u_2 \left[\frac{u_1}{h_1 h_2} \frac{\partial h_1}{\partial x_2} - \frac{u_2}{h_2 h_1} \frac{\partial h_2}{\partial x_1} \right] \\ - 2 \rho \omega_3 u_2 - \frac{\rho \omega^2}{h_1} R \frac{\partial R}{\partial x_1} = - \frac{1}{h_1} \frac{\partial \rho}{\partial x_1} + \frac{\partial}{\partial x_3} \left[\mu \frac{\partial u_1}{\partial x_3} - \rho u'_1 u'_3 \right] \end{aligned} \quad (2)$$

X₂ Momentum Eq. :

$$\begin{aligned} \frac{\rho u_1}{h_1} \frac{\partial u_2}{\partial x_1} + \frac{\rho u_2}{h_2} \frac{\partial u_2}{\partial x_2} + \rho u_3 \frac{\partial u_2}{\partial x_3} + \rho u_1 \left[\frac{u_2}{h_1 h_2} \frac{\partial h_2}{\partial x_1} - \frac{u_1}{h_1 h_2} \frac{\partial h_1}{\partial x_2} \right] \\ + 2 \rho \omega_3 u_1 - \frac{\rho \omega^2}{h_2} R \frac{\partial R}{\partial x_2} = - \frac{1}{h_2} \frac{\partial P}{\partial x_2} + \frac{\partial}{\partial x_3} \left[\mu \frac{\partial u_2}{\partial x_3} - \rho u'_2 u'_3 \right] \end{aligned} \quad (3)$$

X₃ Momentum Eq.:

$$\frac{\partial P}{\partial x_3} = 0 \quad (4)$$

Energy Eq.

$$\begin{aligned} \frac{\rho u_1}{h_1} \frac{\partial I}{\partial x_1} + \frac{\rho u_2}{h_2} \frac{\partial I}{\partial x_2} + \rho u_3 \frac{\partial I}{\partial x_3} = \frac{\partial}{\partial x_3} \left[\frac{\mu}{p_r} \frac{\partial H}{\partial x_3} + \mu \left(1 - \frac{1}{p_r} \right) \times \right. \\ \left. \left(u_1 \frac{\partial u_1}{\partial x_3} + u_2 \frac{\partial u_2}{\partial x_3} \right) \right] - \rho H' U'_3 \end{aligned} \quad (5)$$

Where

I = H - 1/2 (ω² R²) is the rothalpy

H = stagnation enthalpy

ω = blade row rotation speed

R = perpendicular distance from the axis of rotation

±2ρω(v,v) = Represent the corioles force component.

ρω² R = Represent the centrifugal force component

With the velocity component normal to the surface neglected. It is convenient at this point to express the Reynolds stress and turbulent energy transport.

For the steady state there are four types of boundaries in the physical flow domain, inlet, outlet, solid surfaces and periodic boundary. At the inlet of the blade duct the velocity components and turbulent kinetic energy are specified. Turbulence quantities, such as (k) and (ε) are normally not known, but they must be estimated. Usually (k) is set to :-

$$k=(2/3)(T_u.Ux)^2, \tag{6}$$

Where (T_u) is the turbulence intensity and its value ($0.01 < T_u < 0.1$), **Davidson (2003)**.

The dissipation is set to: -
$$\varepsilon_{in} = C_{\mu}^{\frac{2}{3}} \frac{k^{\frac{3}{2}}}{I_c} \tag{7}$$

Where I_c is a characteristic length and is taken as ($0.015S$), where S is the cascade Pitch. Pressure is assumed to be unchanging in the flow direction at the inlet At the exit plane the values of the dependent variables are unknown. Therefore the outlet boundary should be placed far down from the region of interest

NUMERICAL SOLUTION

In the present study we will work on the sequence of two– dimension grids in successive cross – section planes. The equations are formulated in two – dimension rectangular compensation domain ($\xi . \eta$) and are solved numerically over uniform, rectangular grid in that domain. The method of Thompson Thames and Mastin (TTM) is utilized. The method employs the following in- homogeneous Laplace eq. as the generation system and its solving results represented in figures (2), (3) and (4)

$$\begin{aligned} \xi_{xx} + \xi_{yy} &= pc(\xi, \eta) \\ \xi_{xx} + \xi_{yy} &= Q(\xi, \eta) \end{aligned} \tag{8}$$

General conservative form

$$(\rho G1 \phi)_{\xi} + (\rho G2 \phi)_{\eta} = (\Gamma Ja1 \phi_{\xi})_{\xi} + (\Gamma Ja2 \phi_{\eta})_{\eta} + S_{total} \tag{9}$$

The table (1) clarifies equation (9) in general curvilinear coordinate

Equations	Φ	Γ	S_{total}
Continuity	1	0	0
x- momentum	u	$\mu_e = \mu + \mu_t$	$\rho u_1 u_2 k_1 - 2\rho w_3 u_2 - \rho w^2 R \frac{\partial R}{\partial x_1}$ $\rho_e u_{1e} \frac{\partial u_{1e}}{\partial x_1} + \rho_e w^2 R \frac{\partial R}{\partial x_1} - \frac{\partial}{\partial x_3} \left[\mu \left(\left(1 + \frac{\rho \epsilon_m}{\mu} \right) \frac{\partial u_1}{\partial x_3} \right) \right] +$
y- momentum	v	$\mu_e = \mu + \mu_t$	$\rho u_1 k_1 + 2w_3 u_1 - \rho w^2 R \frac{\partial R}{\partial x_2}$ $+ \rho_e u_{1e} K_1 - 2\rho_e w_3 u_{1e} + \rho_e w^2 R \frac{\partial R}{\partial x_2} - \frac{\partial}{\partial x_3} \left[\mu \left(1 + \frac{\rho \epsilon_m}{\mu} \right) \frac{\partial u_2}{\partial x_3} \right] + S_{\xi, \eta}$



Energy	T	$\frac{\mu}{P_l} + \frac{\mu_t}{P_t}$	$\rho w^2 R \left[u_1 \frac{\partial R}{\partial x_1} + u_2 \frac{\partial R}{\partial x_2} + u_3 \frac{\partial R}{\partial x_3} \right] - \frac{\partial}{\partial x_3} \left[\frac{\mu}{P_r} \left(1 + \frac{p_r}{P_{rt}} \frac{\rho \epsilon_m}{\mu} \right) \frac{\partial H}{\partial x_3} + \mu \left(1 - \frac{1}{P_r} \right) \left(u_1 \frac{\partial u_1}{\partial x_3} \right) \right] + S_{\xi, \eta}$
k-equation	k	$\mu + \frac{\mu_t}{\sigma_k}$	$[G_k - \rho \epsilon] + S_{\zeta, \eta}$
ϵ - equation	ϵ	$\mu + \frac{\mu_t}{\sigma_\epsilon}$	$\left[\frac{\epsilon}{k} (C_{\epsilon 1} G_k - C_{\epsilon 2} \rho \epsilon) \right] + S_{\zeta, \eta}$

The Nusselt Number

For forced convection of a single-phase fluid

$$q''_w = h(T_w - T^*) \dots\dots\dots(12)$$

where **h** is called the heat transfer coefficient, with units of W/m^2 , heat flux would be entirely due to fluid conduction through the layer:

$$q''_w = k(T_w - T^*)/L \dots\dots\dots (13)$$

We define the Nusselt number as the ratio of these two:

$$NuL = \frac{q''_w (convection)}{q''_w (conduction)} = hL/k. \dots\dots\dots (14)$$

Sequence of solution steps

The overall solution procedures can be listed as follows:

- 1) An initial guess is given for all variables in the field of interest.
- 2) The proper boundary conditions are specified for all dependent variables.
- 3) The discretised momentum equation is solved to obtain the covariant velocity components.
- 4) Then the pressure correction equation is solved to obtain pressure correction field.
- 5) The pressure correction is then used to correct pressure fields using equation
- 6) Then the velocity and density fields are corrected using equation
- 7) The other dependent variables such as turbulence and energy equations are solved.
- 8) The density is calculated using the new temperature and pressure fields.

The whole procedure is repeated from step three until a convergent solution is obtained

RESULTS and Discussion

In the beginning of running the computer program we solve the governing equation for simple rectangular duct as represented in figure (5) and (6), the turbulent modeling was also adopted for the duct flow and we can see the turbulent kinetic energy in duct flow in Fig (7) and (8) The velocity contours of the present work were made for three different values of Reynolds number.

The first Reynolds number was 5000 and its (U) velocity contours is presented in fig (9), in this figure we can see the uniform velocity at the entrance of the domain, this uniform flow is because the flow coming from uniform source this source is the stationary blade which work as a nozzle to increase the velocity and give the flow more stability. The flow velocity increases uniformly inside the domain and reaches a value over the entrance velocity in the region at the mid chord of the blade and also we see the same in Figures (10) and (11).

The V – velocity contour for the three Reynolds number are plotted in figures (12) to (14), which indicates a uniform velocity at the entrance and it decreases towards the exit

The second important variable in the present work is the pressure distribution in the space between the rotating blades. Figures (18), to (20) show the predicted static pressure distribution at different plane for Reynolds number equal (5000, 10000, 100000) respectively, we can see higher pressure distribution near the pressure surface than that close to suction surface this is due to the positive inclination (angle of attack) of the blades

The figures (21) to (23) show the dimensionless turbulent kinetic energy for Reynolds number (5000, 10000, 100000) respectively we observe the minimum value of turbulent kinetic energy near wall and increases toward the center. The turbulent kinetic energy be minimum near wall where the flow velocity is minimum.

Depending on the velocity value appear during solving the governing equation we can get the velocity profile. These profiles shown in Figures (25) to (28) and for Reynolds Number (100000 and 10000) for different locations in the core line for the blades. We fix the points where the velocity reach the max flow velocity we get the boundary layer form as show the Fig (29)

After predicting the boundary layer profile we fix the point of velocity equal to 0.99 maximum velocity at the suction surface these points provide us with the boundary layer, this process done for 1500 rad/s rotating speed. This procedure repeated for another rotating speed (1800 rad/s, 1900 rad/s) to see how dose the rotating speed affects the boundary layer behavior, the new boundary layer form presented in fig(30). we see in this figure that increases in rotating speed have bad effect on the boundary layer form specially at ($x/c > 0.9$)

The figures (31 to 34) show the temperature distribution developing. For the case of constant upper blade temperature and thermal insulated lower blade for Reynolds ($Re = 50,000$), we observe that the temperature increases in the direction of the flow and the temperature decreases in the vertical direction. In the middle of the geometry we observe the decrease is greater then decreases slightly toward the lower wall.

CONCLUSION REMREKS

The present work solves the fluid flow and heat transfer between rotating impulse turbine blades. The following conclusions are drawn from the obtained results; the flow velocity increases uniformly inside the calculation domain and reaches a value over the uniform entrance velocity in the region at the mid chord of blade. the velocity vectors are more uniform at the middle section than at the entrance and they become unstable at the trailing edge section. the boundary layers are more uniform at the pressure side than at the section side.

High pressure is observed near the pressure side than thus close to suction side, and denser pressure contours near the leading edge of the pressure side is also observed. A minimum value of turbulent kinetic energy is observed near the wall and it increases towards the center. Increase in rotational speed causes a deformation and increase in boundary layer thickness. A normal temperature distribution is obtained, and the large velocities on the suction side cause streamwise vortex that



continuously heat transfer. The Nusselt number is maximum at the entrance section and decreases with the flow direction until it reach approximately constant value. An acceptable agreement was obtained with previous published numerical and experimental results,

REFERENCES

Davidson, L., 2003, "An Introduction to Turbulence Models", Chalmers University of Technology, Department of Fluid Dynamics

Dorfman A.S. (1996) "Advanced Calculation Method for the Surface Temperature of Turbine Blade" Journal of heat Transfer 48(1): pp.18 – 22.

Gogzeh, M.M. (2000) "Three Dimensional Turbulent flow Prediction between Two Axial Compressor Stator Blades Using Body Fitted Coordinate System "PhD. – theses. Mechanical Dep. University of Baghdad

Hoffmann, K. A., 1989, "Computational Fluid Dynamics for Engineers", Engineering Education System

K. M. Bernhared (2000) "Experimental Study of Effusion Cooling" Department of Thermo and fluid Dynamic Chalmers University of Technology. Sweden.

Koya M., and S. Kotake (1985) " Numerical Analysis of Fully Three – dimensional peridic flow Though a Turbine Stage" ASME Journal of Engineering for Gas Turbine and Power, Vol.107, No.4, pp. 945 - 952

Patankar, S. V., 1980, "Numerical Heat Transfer and Fluid Flow" Hemisphere, McGraw-Hill, New York.

Versteeg, H. K. and Malalasekera, W. (1995). An Introduction to Computational Fluid Dynamics, the finite volume method. Longman Scientific and technical

W. T. Thompkins (1982)" A – Quasi Three Dimensional Blade Surface Boundary Layer Analysis for Rotating Blade Rows" journal of Engineering and Power. Vol. 104. pp.439 – 448.

Table 2 definition of symbols used in present work

Symbol	Description	Units
C	Chord of the blade	m
C_μ	Constant in turbulence model	
$C_{\varepsilon 1}$	Constant in turbulence model	
$C_{\varepsilon 2}$	Constant in turbulence model	
C_x	Axial chord of the blade	m
G_1	Contravariant velocity in ζ direction	m/s
G_2	Contravariant velocity in η direction	m/s
G_3	Contravariant velocity in Z direction	m/s
J	Jacobian transformation	
k	Kinetic energy of turbulence	
MUE	Turbulent Viscosity	

P	Pressure	N/m^2
R	Perpendicular distance	m
Re	Reynolds number ($Re = \rho_{\infty} U_{\infty} C_x / \mu$)	
S	Cascade pith	m
S_{ϕ}	Source term of ϕ	
$S_{\zeta\eta}$	Source term due to nonorthogonalit y	
S_{total}	Total source terms	
t	Time	s
T	Temperature	$^{\circ}C$
T_u	Turbulence intensity	
u	Velocity component in x direction	m/s
v	Velocity component in y direction	m/s
w	Velocity component in z direction	m/s
x	Axial coordinate in the physical domain	
Z	Spanwise coordinate in the computational domain	
ω	Rotating speed	Rad/sec

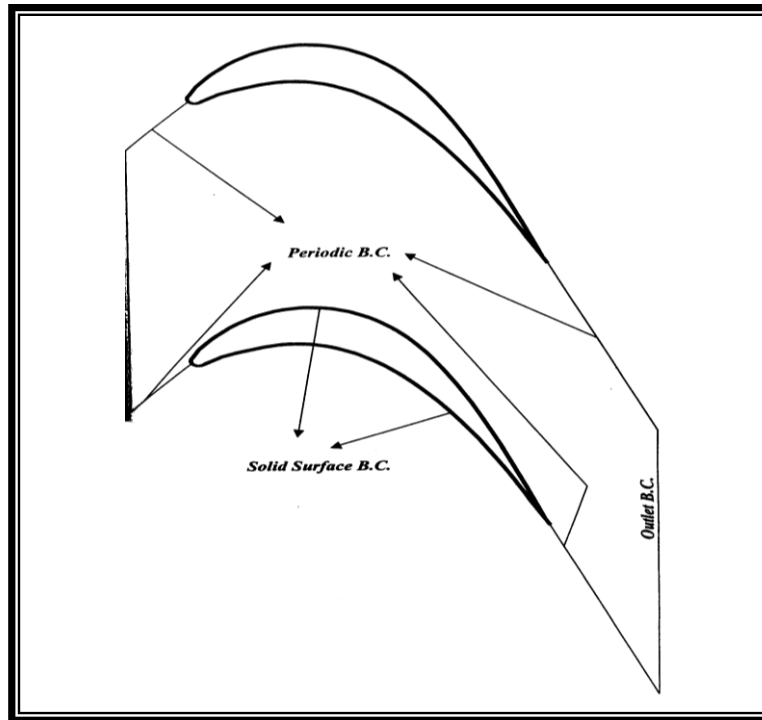


Fig (1) Two Dimension Blade

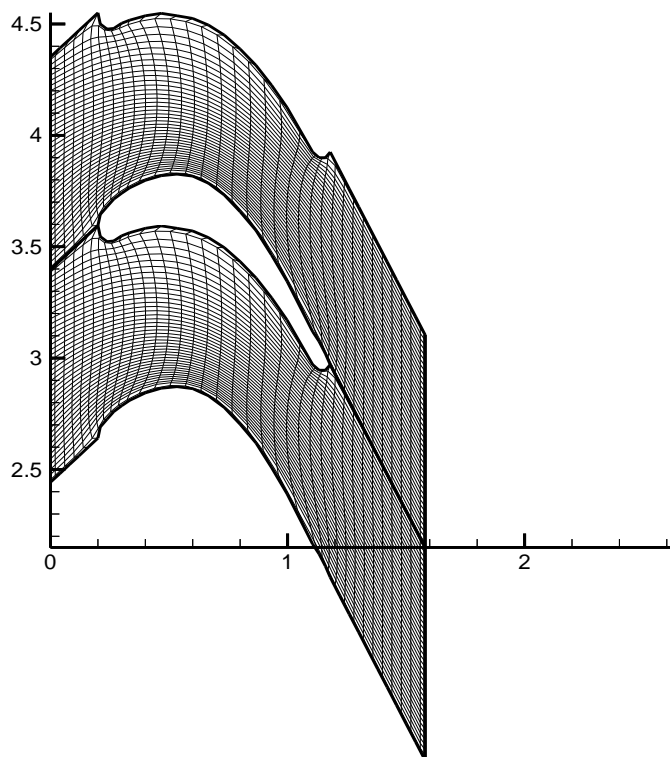


Fig (2) elliptical grid system for (M x N = 33x21)

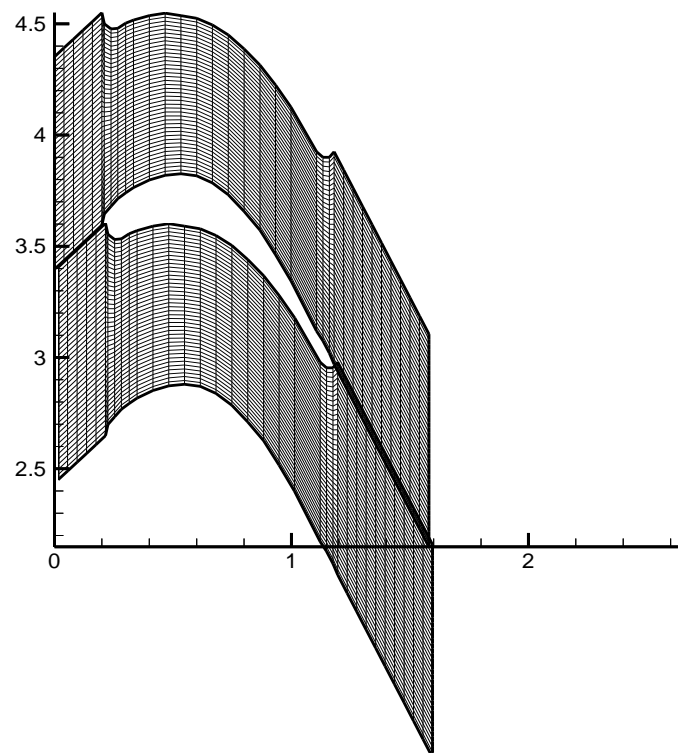


Fig (3) Algebraic Grid system for (MxN = 33 x 21)

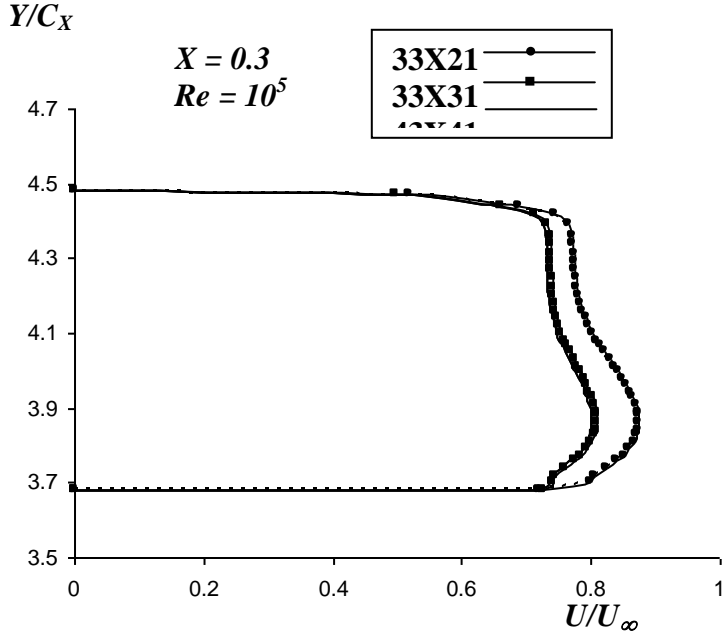


Fig.4: Ensemble – Averaged Velocity Profile at $X = 0.3$ and $Re = 10^5$ for Three Grids

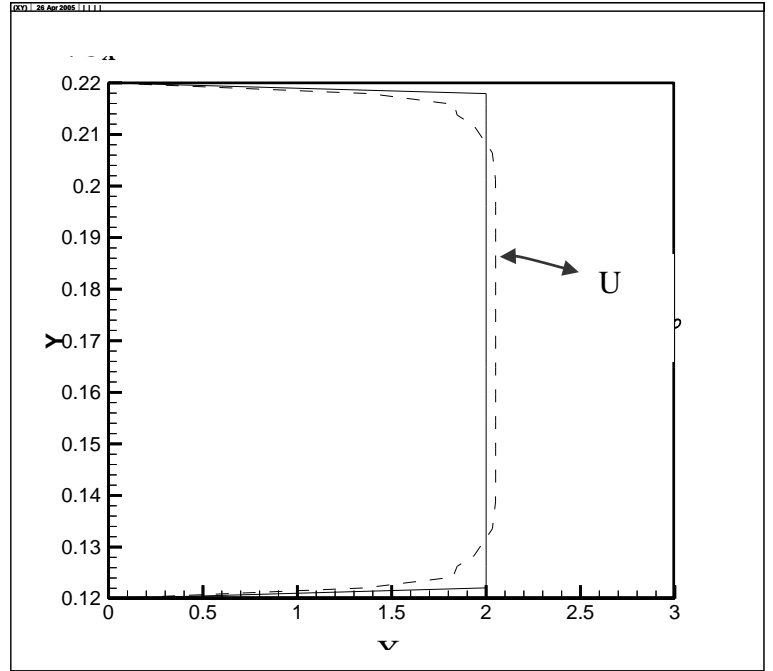


Fig. 5: Velocity profile for duct flow

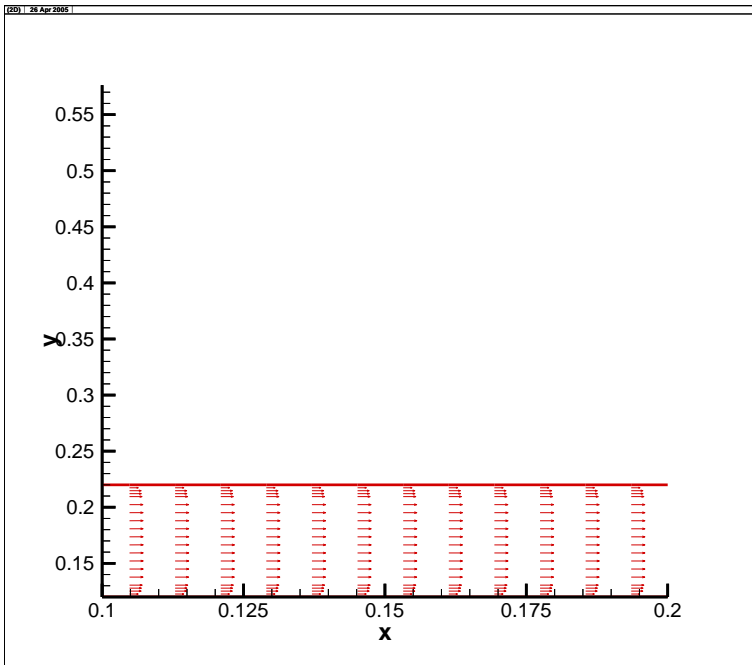


Fig.6: Velocity Vector for duct flow

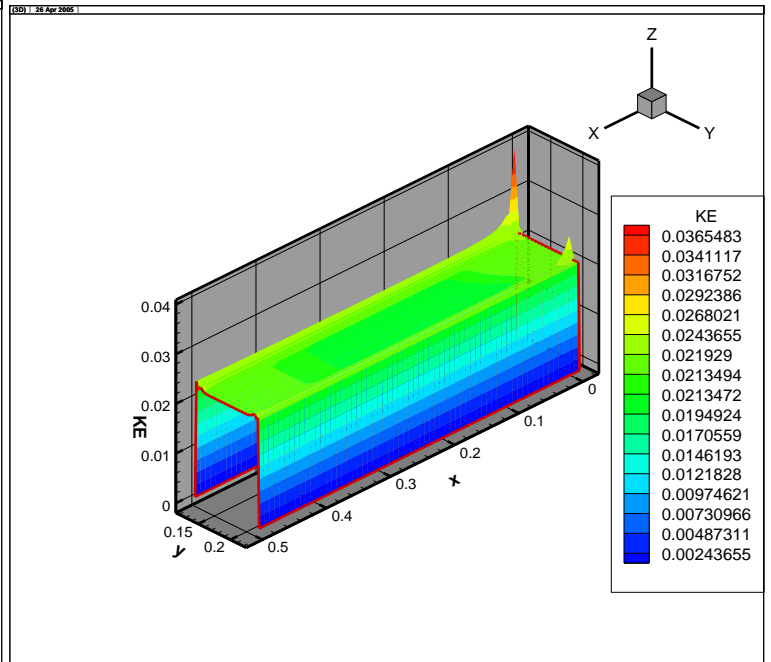


Fig. 7: KE for duct flow

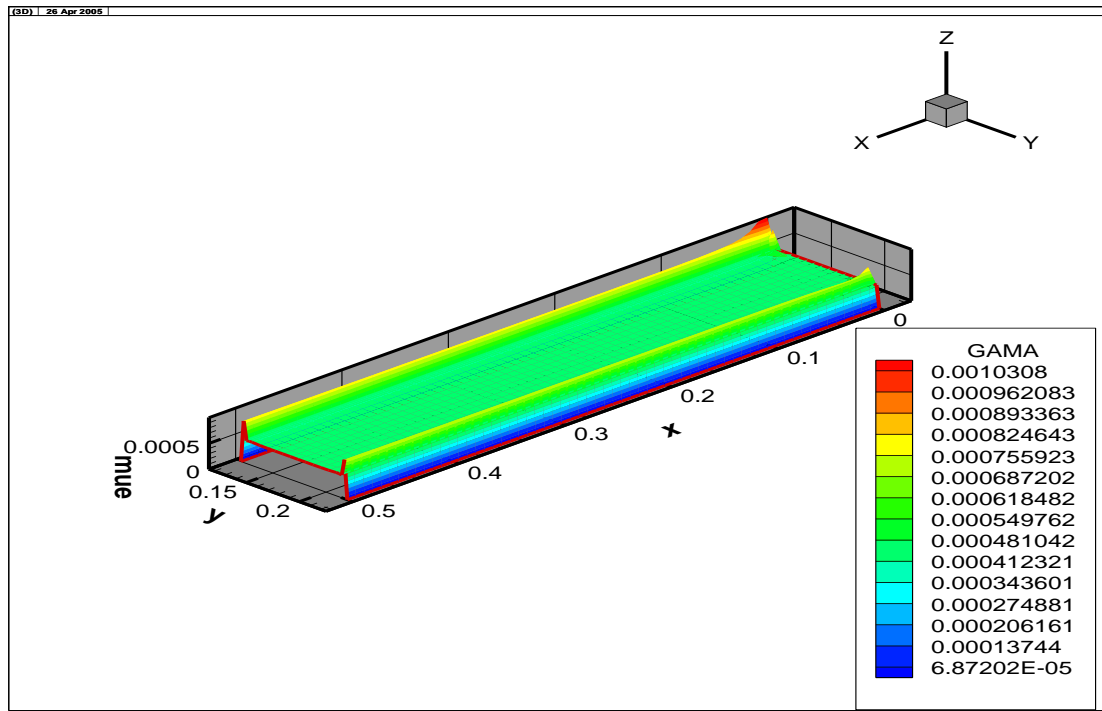


Fig. 8: MUE for duct flow

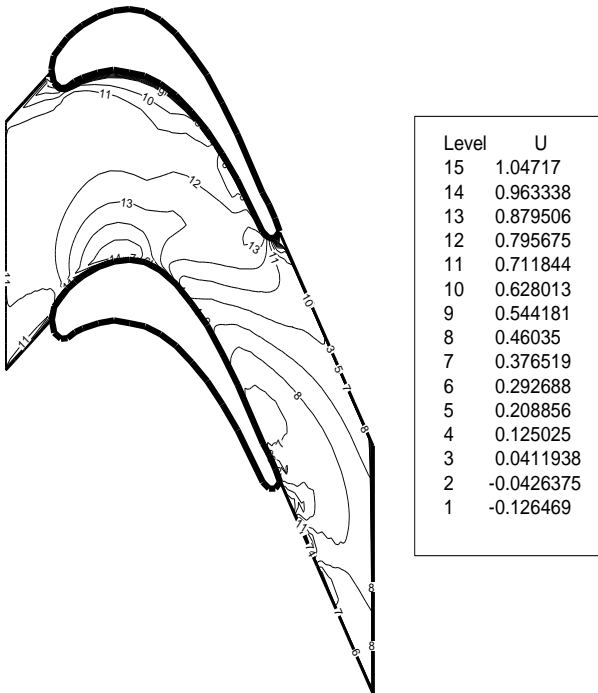


Fig. 9: U Velocity Contour at Re= 5000

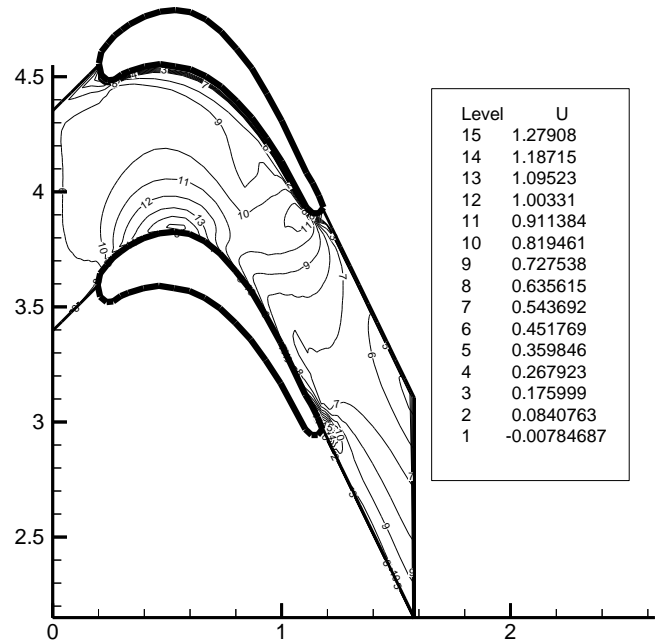


Fig. 10: U - Velocity Contour at Re = 10000

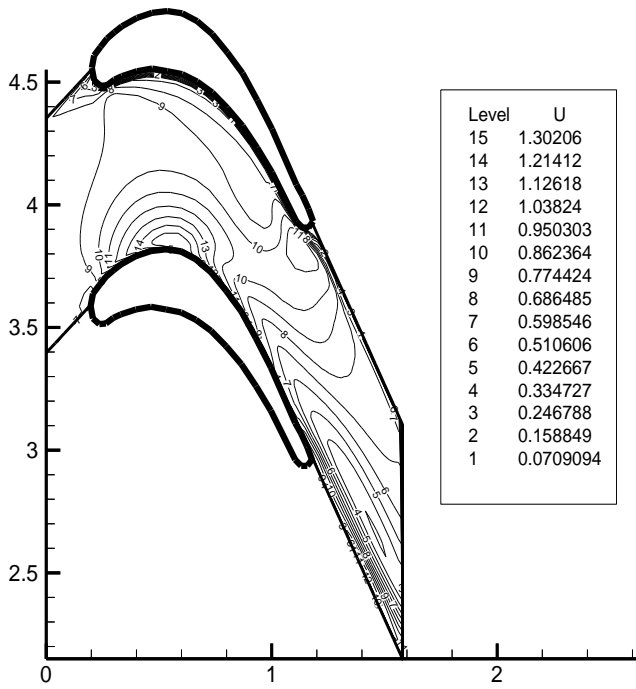


Fig. 11: U - Velocity Contour at Re = 100000

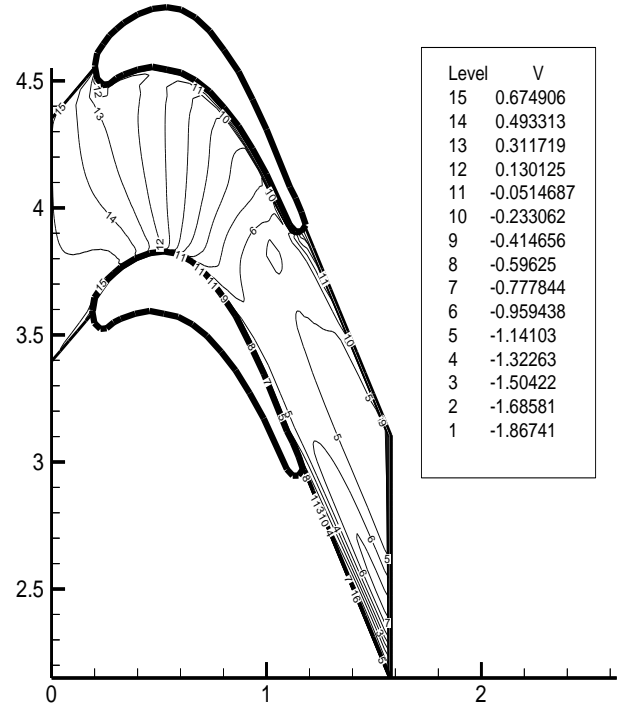


Fig. 12: V - Velocity Contour at Re= 5000

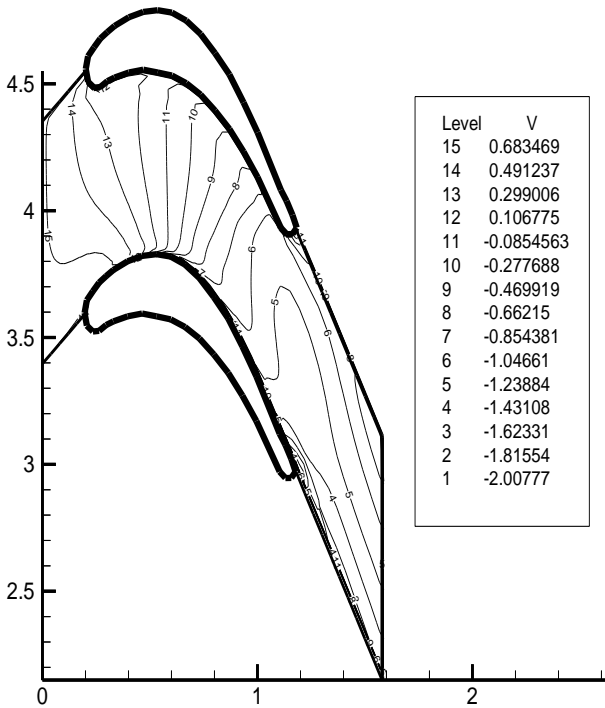


Fig. 13: V - Velocity Contour at Re= 10000

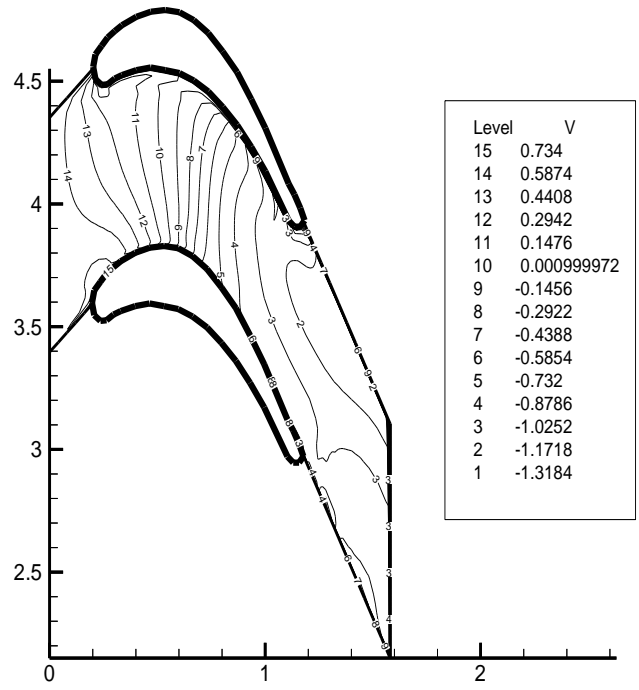


Fig. 14 V - Velocity Contour at Re= 100000

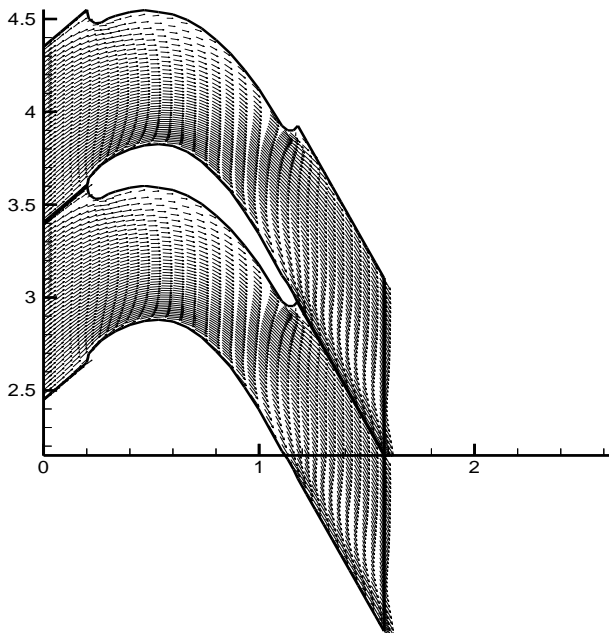


Fig. 15: U Velocity Vector at Re = 5000

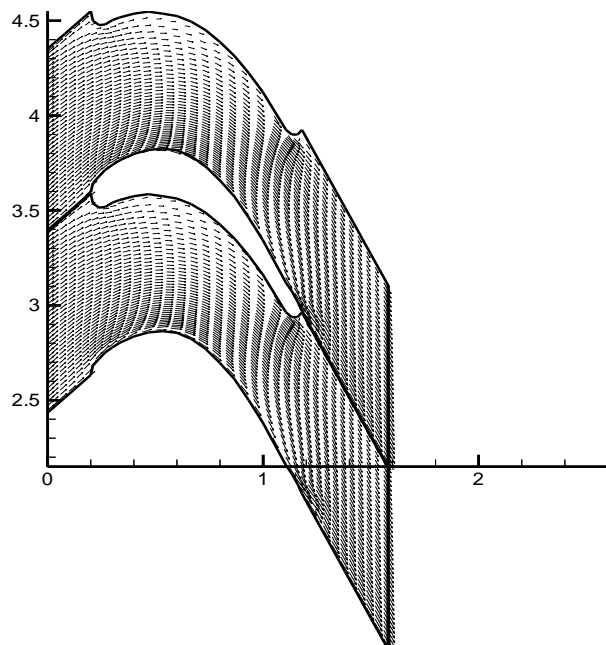


Fig. 16: U Velocity Vector at Re = 10000

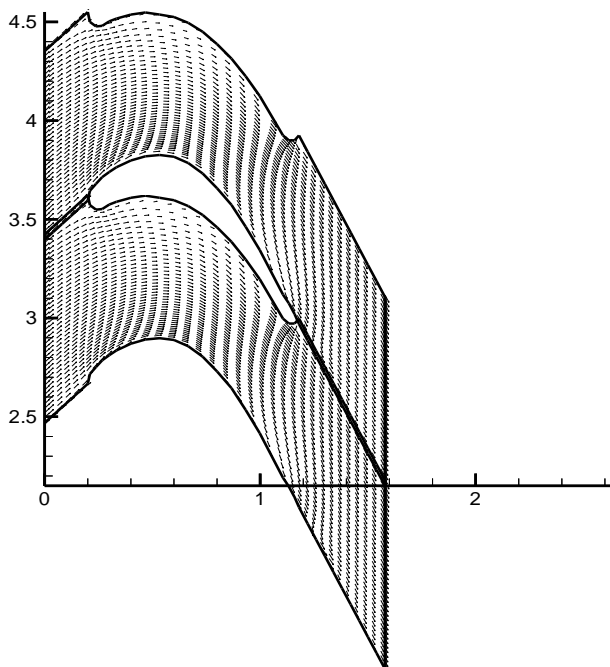


Fig. 17: U Velocity Vector at Re = 100000

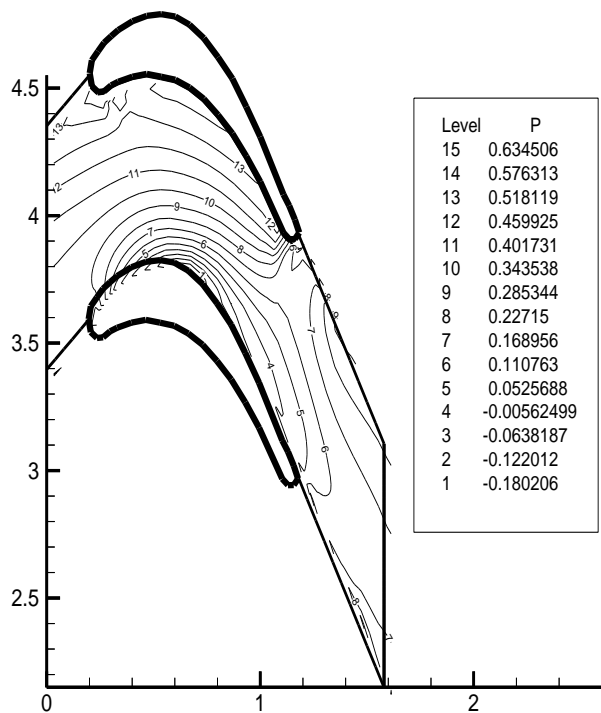


Fig. 18: Pressure Contour at Re = 5000

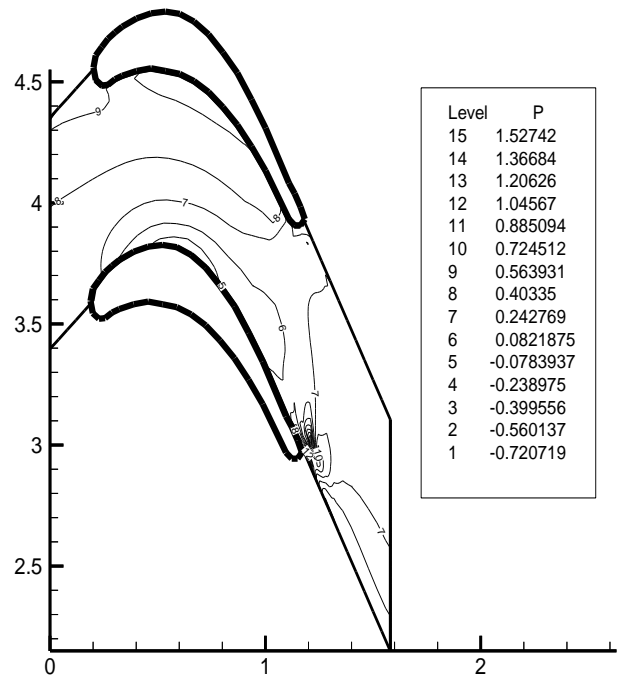
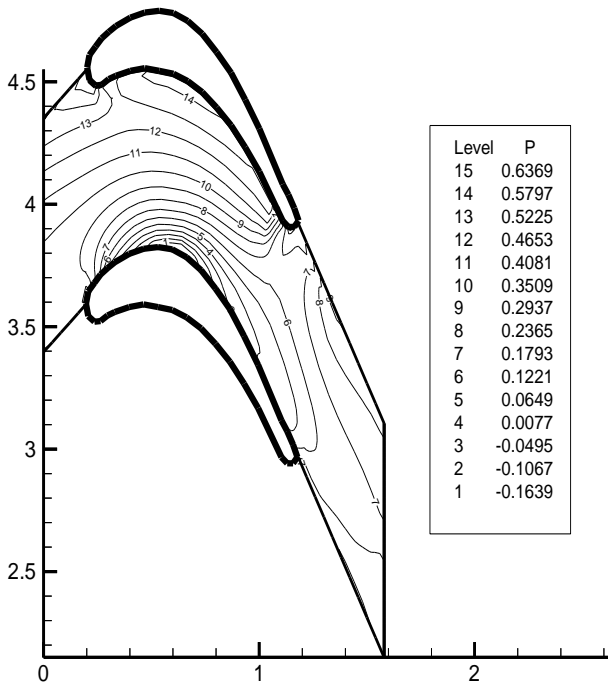


Fig. 19: Pressure Contour for Re = 10000

Fig. 20: Pressure Contour for Re = 100000

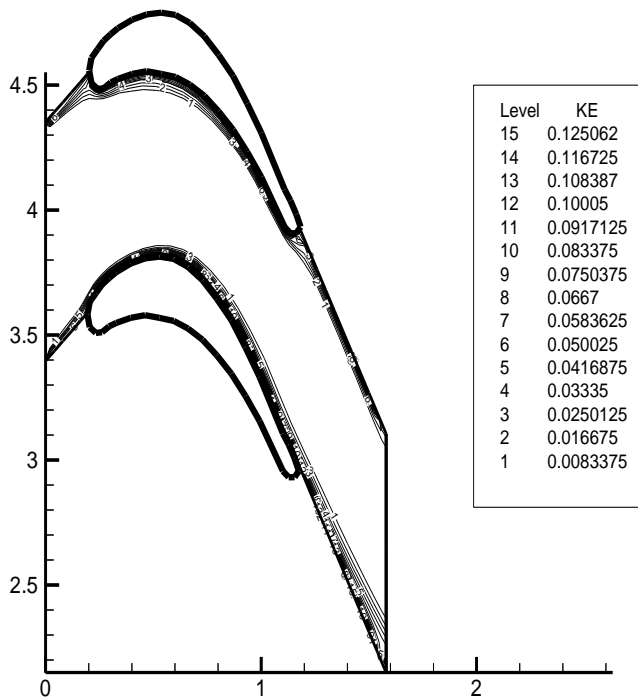


Fig. 21: KE Contour at Re = 5000

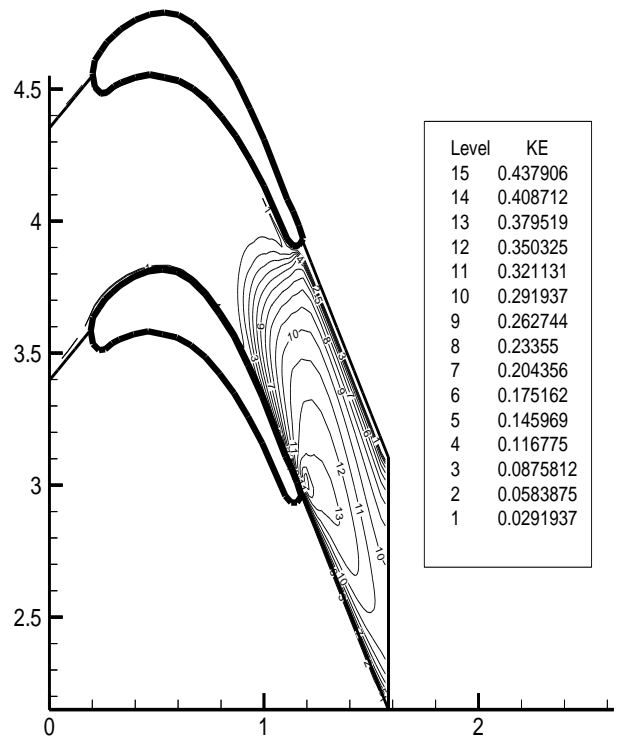


Fig. 22: KE Contour at Re = 10000

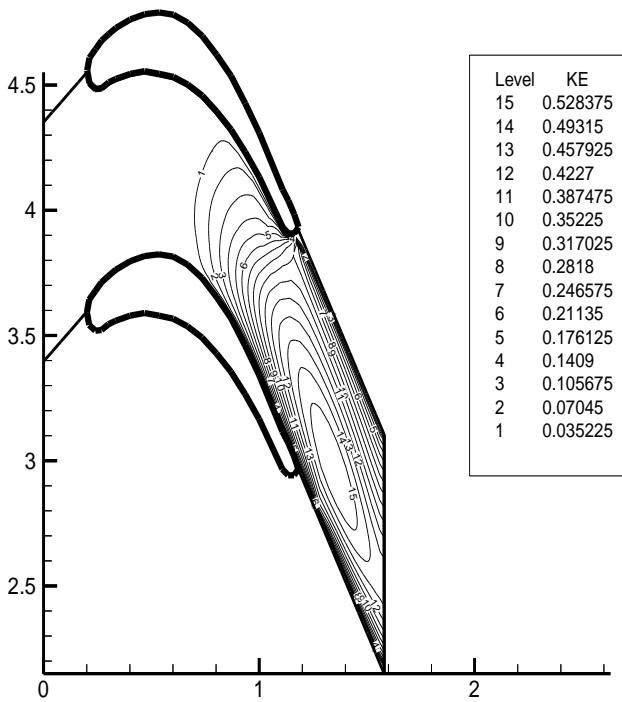


Fig. 23: KE Contour at Re = 100000

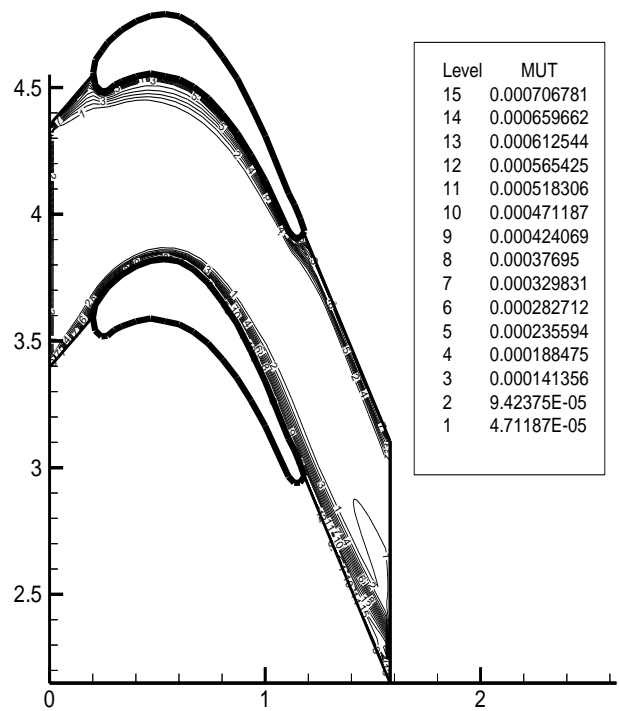


Fig. 24: MUT Contour at Re = 100000

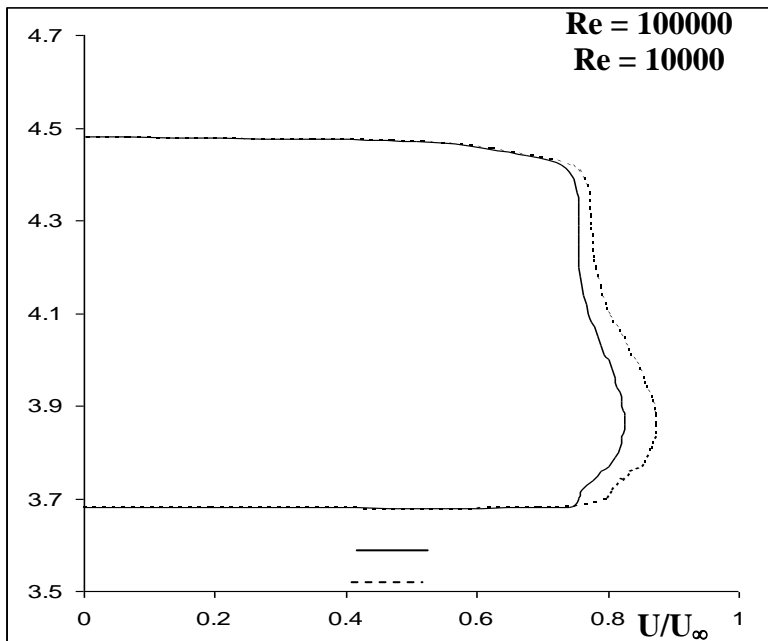


Fig. 25: Velocity profile at (X/C)= 0.33

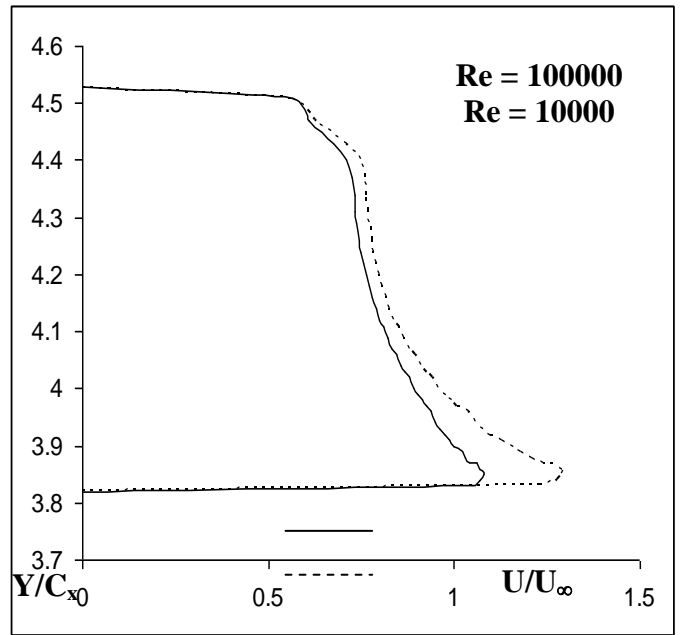


Fig. 26: Velocity profile at (X/C)= 0.6

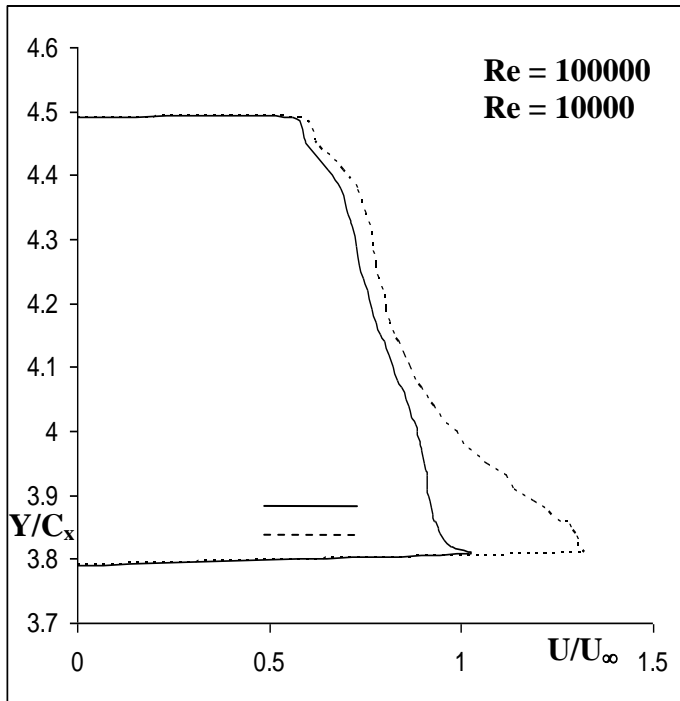


Fig. 27: Velocity profile at $(X/C) = 0.8$

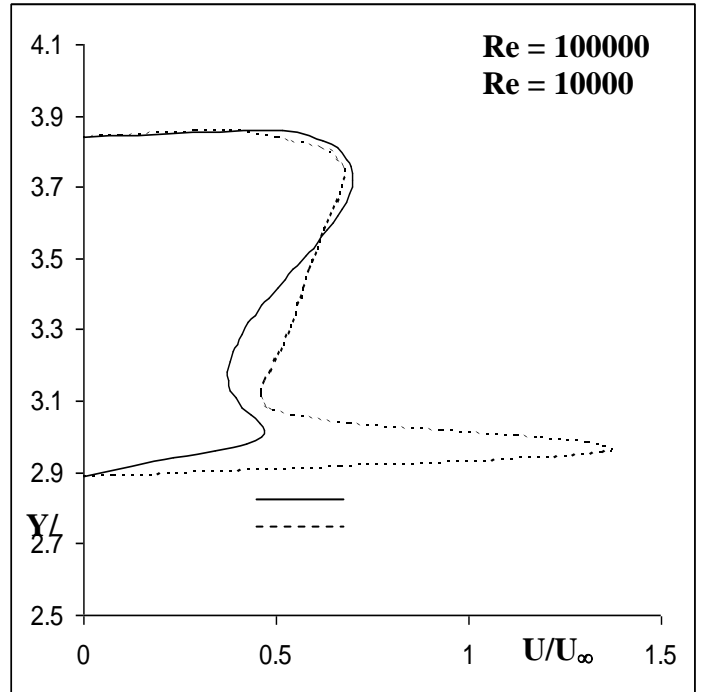


Fig. 28: Velocity profile at $(X/C) = 1.22$

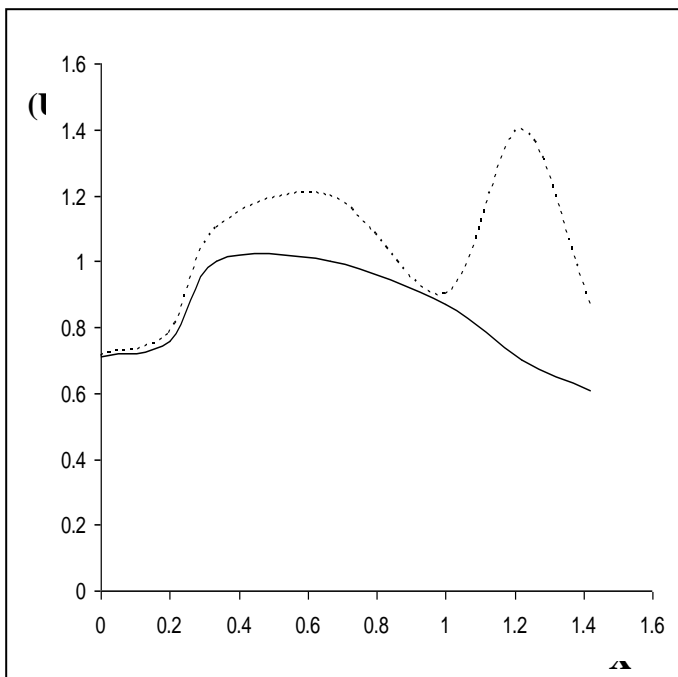


Fig. 29: Boundary Layer Form

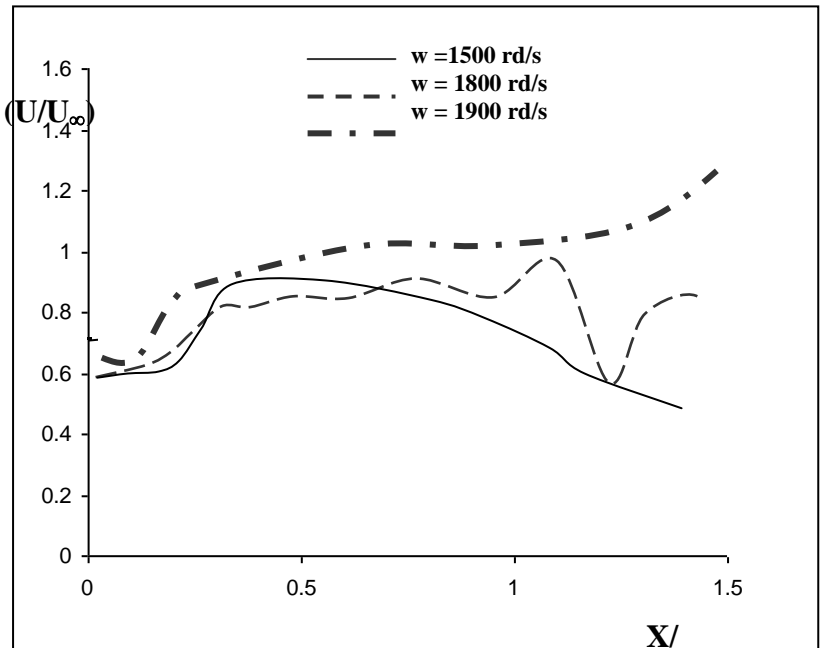
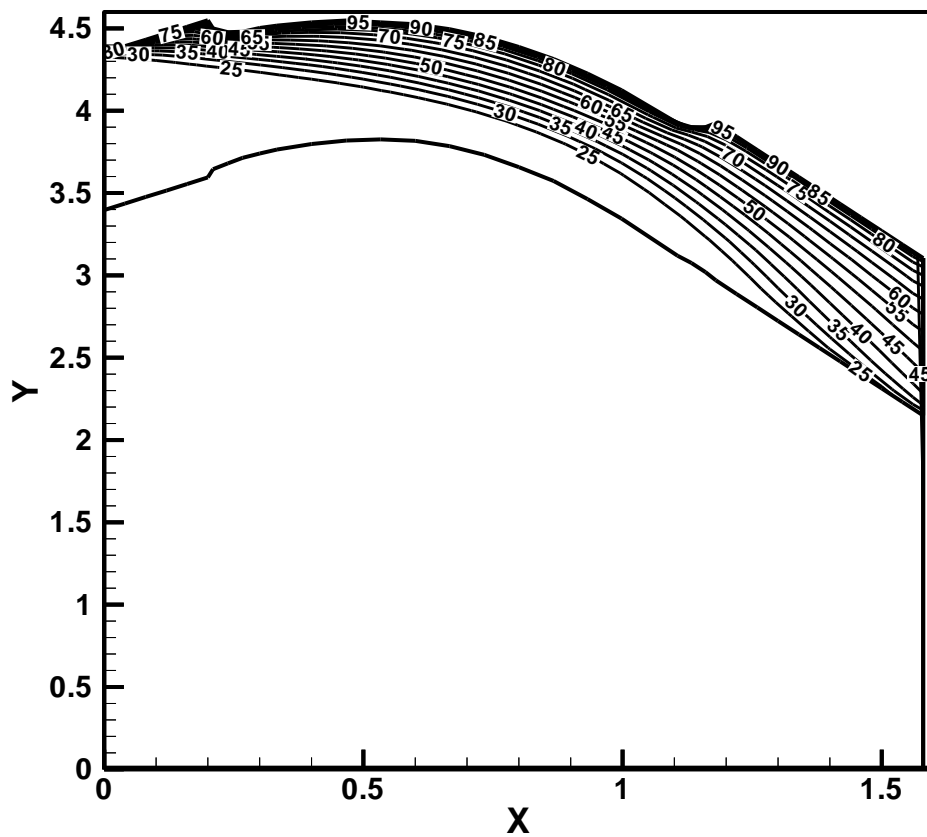
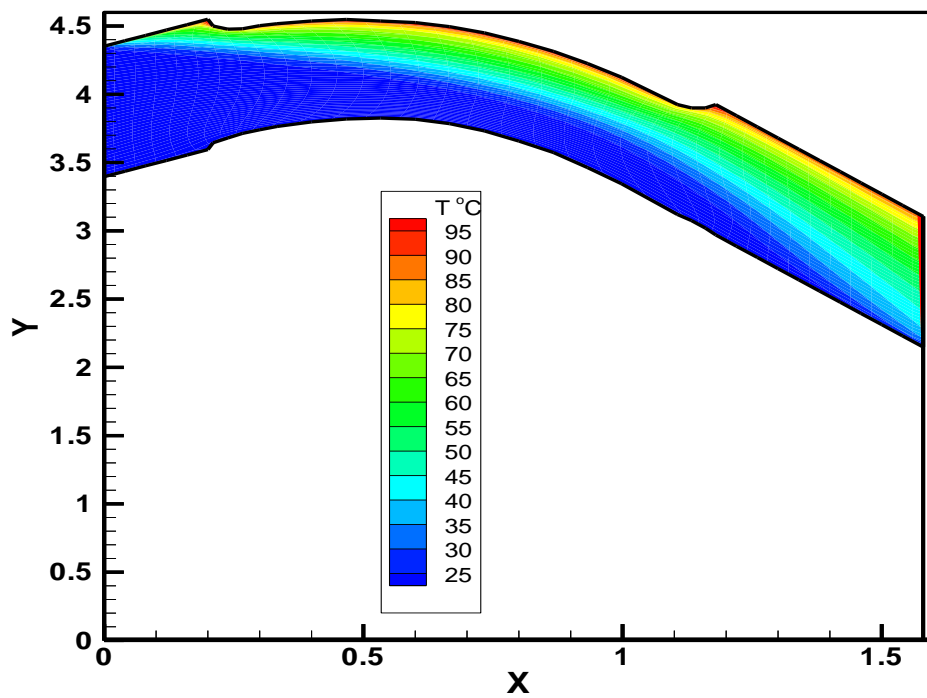


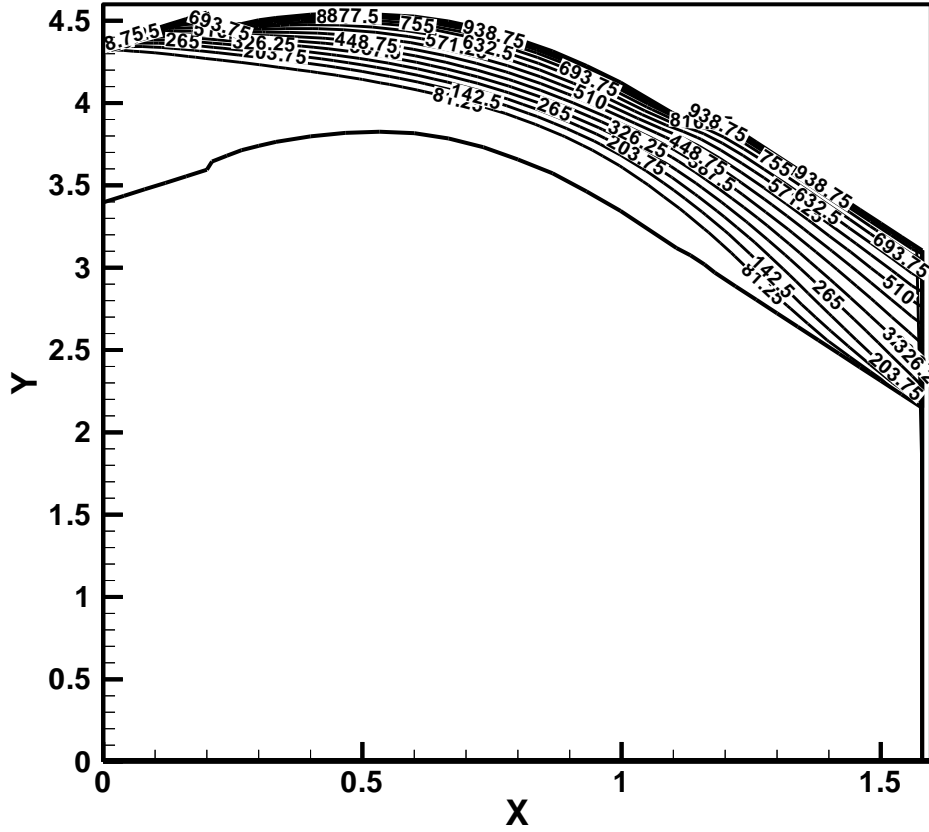
Fig. 30: Boundary Layer Form for Different Rotating Speed



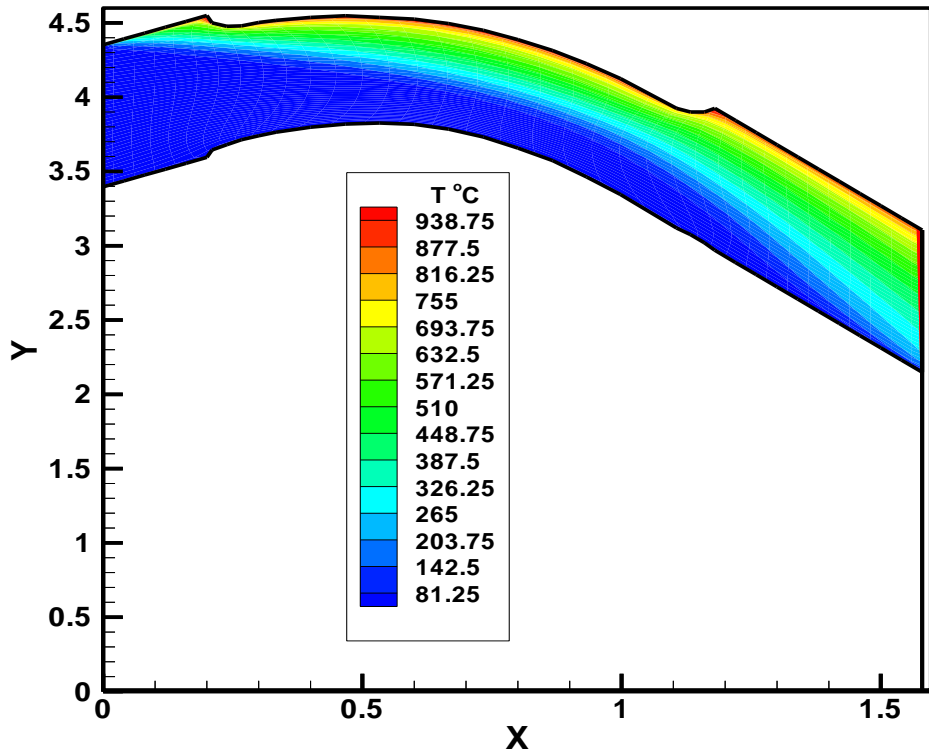
Figure(31): Contour (Lines) of temperature distribution for $Re=50,000$ and constant wall temperature $T_w=100\text{ }^\circ\text{C}$



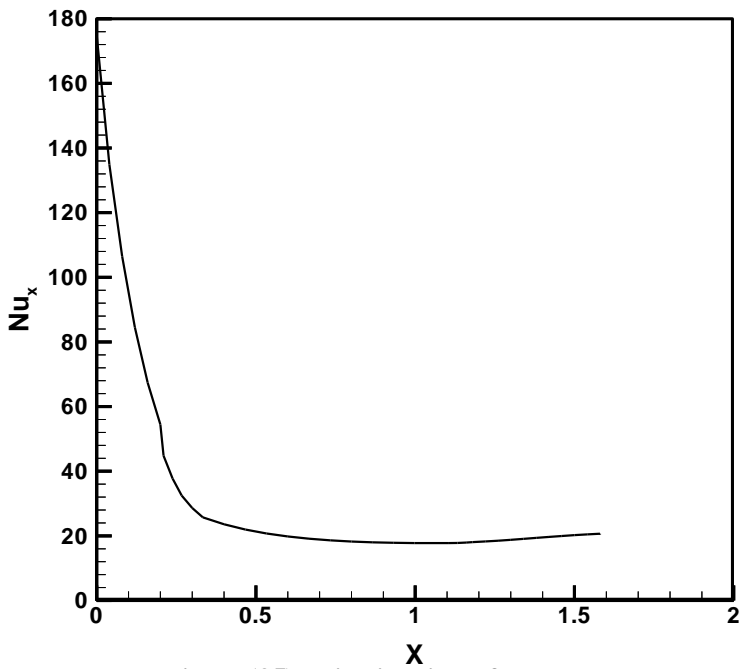
Figure(32): Contour (flood) of temperature distribution for $Re=50,000$ and constant wall temperature $T_w=100\text{ }^\circ\text{C}$



Figure(33): Contour (Lines) of temperature distribution for $Re=50,000$ and constant wall temperature $T_w=1000\text{ }^\circ\text{C}$



Figure(34): Contour (flood) of temperature distribution for $Re=50,000$ and constant wall temperature $T_w=1000\text{ }^\circ\text{C}$



Figure(35): Distribution of Local Nuselt Number for Re=50,000 and $T_w=1000\text{ }^\circ\text{C}$

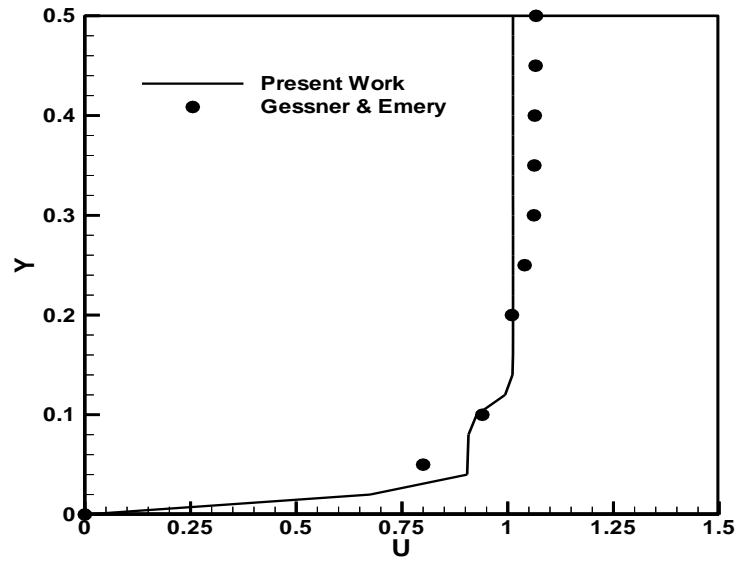


Fig.36: Boundary Layer Form comparison for duct flow

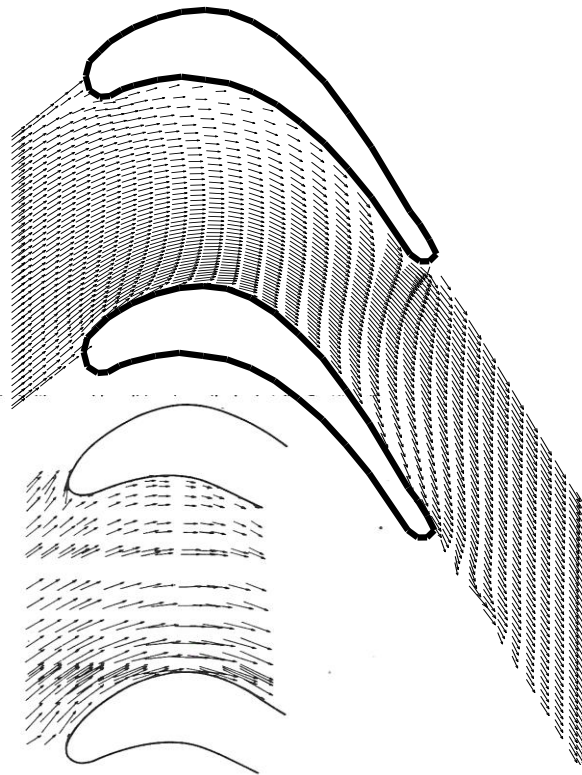


Fig. 37: Comparison Velocity Vector Re=5.9x100000 with Hah 1984